CHAPTER Three

Chapter three describes the synthesis and characterization of tetrahydrofuran and hydrogen peroxide mediated nanocrystalline nickel-iron hexacyanoferrates nanoparticles. As synthesized Ni-Fe HCFs were well stable shows the different electrochemical behaviour depending on the molar ratio of Ni:Fe. Ni-Fe HCFs was further characterized by various techniques. As synthesized nickel-iron hexacyanoferrates was further used for the detection of hydrogen peroxide homogeneously and hydrazine as heterogeneously.

1 THF and H_2O_2 mediated synthesis of nanocrystalline Ni-Fe HCFs and its analytical applications

1.1 Introduction

Transition metal hexacyanoferrate (MHCF) have gained a huge interest among scientist due to its unique physical and chemical properties which is exploited in the field of electrochemistry, environmental and medical science, electrode material in rechargeable batteries, molecular magnets and many more. When –CN group surrounds iron (Fe) metal centre then it is known as Prussian blue but when –CN group coordinates two metal centres and –Fe is one of the member then it is known as Prussian blue analogue [(Neff 1978)]. Prussian blue and its analogues are generally synthesized either by co-precipitation or by electrodeposition method. Potential viability of mixed metal hexacyanoferrate have directed extensive investigation involving different combination of transition metals like Co–Fe [(Yu *et al.* 2013)], Ni–Co [(Kulesza *et al.* 1999; Safavi *et al.* 2011)], Cu–Co [(Abbaspour and Ghaffarinejad 2008)], Ni–Pd [(Kulesza *et al.* 2000)] and Ni–Fe [(Ghasemi *et al.* 2015; Salimi and Abdi 2004)]. The electrocatalytic response and electrochemical behaviour of metal hexacyanoferrate analogues are relatively better as compared to that of single metal hexacyanoferrate due to the presence of another transition metal in the cubic structure along with iron and have been exploited in electrochemical energy storage [(Ghasemi *et al.* 2015)] , electrochemical sensing of glutathione and hydrogen peroxide [(Pandey and Pandey 2012b, 2013a)], dopamine [(Zhou *et al.* 1996)] and many more. The practical applications of these metal hexacyanoferrate analogues are restricted due the insolubility of the material for further processing in desired applications. In addition to that precise control over nanogeometry, crystallinity and catalytic activity of such material are another challenging task of research findings restricting the wider application of such materials. Therefore, there is a need of a novel synthetic approach that enable the synthesis of water soluble metal hexacyanoferrate analogues at room temperature in a rapid and cost effective manner. Meeting these requirements, we have recently investigated the synthesis of processable Prussian blue through the active participation of 3-

aminopropyltrimethoxysilane (3-APTMS) and cyclohexanone [(Pandey and Pandey 2013c)] displaying excellent electrochemistry with the electron transfer rate constant in the order of 32 s^{-1}. Similar reaction protocol has subsequently been exploited for the synthesis of super peroxidase mimetic mixed metal analogue nanoparticles [(Pandey and Pandey 2013a)]. Although, such method yielded the synthesis of processable mixed metal hexacyanoferrate nanoparticles, the use of 3-APTMS enabled auto hydrolysis, condensation and polycondensation leading to the formation of –Si–O–Si– linkage during prolonged operation of the materials. Fortunately, we succeeded in replacing the use of 3-APTMS by tetrahydrofuran hydroperoxide (THF-HP) that enabled controlled synthesis of water soluble Prussian blue nanoparticles (PBNPs) at room temperature [(Pandey and Pandey 2014a)]. Although the use of THF-HP allowed the synthesis of processable PBNPs, the synthesis of mixed metal hexacyanoferrate remained in question due to relatively slow process of Prussian blue formation in the presence of THF-HP. In addition to that the availability of THF-HP for cost effective synthesis of such material has been another issue since commercial availability of the same is rare and laboratory preparation of material is also tedious. Accordingly, we attempted to find out the way for controlling the synthesis of water soluble mixed metal hexacyanoferrate nanoparticles. We found that the use of tetrahydrofuran and hydrogen peroxide, both of them are common laboratory reagents; efficiently convert the synthesis of nickel–iron hexacyanoferrate within < 30 minutes at 60 °C displaying excellent nanogeometry, crystallinity and processability for practical applications. Accordingly, the findings on: (i) tetrahydrofuran, hydrogen peroxide, and nickel sulphate based conversion of potassium ferricyanide into its nickel–iron hexacyanoferrate (hereinafter Ni–Fe HCF), (ii) structural and elemental characterization of as synthesized Ni-Fe HCFs, (iii) homogeneous catalysis of as synthesized Ni-Fe HCFs towards hydrogen peroxide determination, and (iv) electrocatalytic ability of as synthesized Ni-Fe HCFs modified electrode in hydrazine sensing are studied in this chapter-3.

1.2 Experimental

1.2.1 Material and Methods

All the reagents were of analytical grade and used without further purification. Potassium ferricyanide [$K_3Fe(CN)_6$], hydrogen peroxide (H_2O_2), and nickel sulphate ($NiSO_4$) were purchased from Merck, India. O-dianisidine, graphite powder (particle size 1–2 μm), nujol oil (density 0.838 g ml^{-1}), and hydrazine hydrate were obtained from Sigma Aldrich Chemical Co. India. Tetrahydrofuran (THF) was purchased from Alfa Aesar, India. The water used in all the experiments was double distilled water (Alga water purification system).

1.2.2 Synthesis of nanocrystalline Ni-Fe hexacyanoferrates (Ni-Fe HCFs)

Synthesis of Ni–Fe HCF involves mixing of optimized concentration of $K_3[Fe(CN)_6]$, THF, H_2O_2 and $NiSO_4$ and allowing the reaction to proceed for 30 minutes at 60 °C. In a typical process, 70 μl $K_3[Fe(CN)_6]$ (0.05 M), 10 μl of THF (12.33 M) and 20 μl of H_2O_2 (3.5 M) were mixed thoroughly in a glass vial. To this, 15 μl $NiSO_4$ (0.05 M) was added, mixed vigorously and kept at 60 °C for 30 min in an oven. A yellow colour solution was turned into blue indicating the formation of Ni– Fe HCF. The formation of such material was also made using variable molar ratio of Ni and Fe referred as vials A, B, C, D, E and F as shown in Table.3.1.

Table.3.1. Synthesis of Ni-Fe HCF as a function of variable composition of $K_3[Fe(CN)_6]$ and $NiSO_4$.

Vial	$K_3[Fe(CN)_6]$ (mol L^{-1})	THF (mol L^{-1})	H_2O_2 (mol L^{-1})	$NiSO_4$ (mol L^{-1})	Ni-Fe HCF formation
A	0.035	1.20	0.7	-	(Deep Blue) PB formation
B	0.035	1.20	0.7	0.001	Blue
C	0.035	1.20	0.7	0.003	Blue
D	0.035	1.20	0.7	0.006	Light Blue
E	0.035	1.20	0.7	0.009	Light Blue
F	0.035	1.20	0.7	0.013	Green

1.2.3 Structural characterization of Ni-Fe hexacyanoferrates (1:5)

The formation of Ni–Fe HCFs having Ni–Fe molar ratio of 1:5 was confirmed by UV–Vis spectroscopy, Fourier Transformation-Infrared spectroscopy, X-ray diffraction analysis and Energy Dispersive Spectroscopy.

Hitachi U-2900 spectrophotometer was used for the measurement of absorbance spectra. Fourier transformation infrared spectroscopy (FT-IR), X-ray diffraction analysis (XRD) and energy dispersive spectroscopy analysis (EDS) were done using the powder of Ni–Fe HCF.

Powder was obtained by keeping the solution of Ni–Fe HCF at 60 °C for an overnight in an oven. A Perkin Elmer spectrum 100 spectrophotometer was used for the FTIR analysis.

The X-ray diffraction pattern was obtained on a Rigaku miniflex II diffractometer using nickel filtered CuKα (λ = 1.506 Å) radiation. X-ray diffraction analysis was performed by powder of Ni-Fe HCFs which was obtained by keeping solution of Ni-Fe HCFs at 60 °C in vacuum oven for an overnight. The crystallite size was

calculated using Debye–Scherrer formula [(Zheng *et al.* 2007)] as described in chapter-2..

Atomic Force Microscopy (AFM) was conducted on AFM–STM model PRO 47, NT-MDT, Russia, and the samples were made by drop casting the Ni–Fe HCF solution on to the cleaned glass substrate. Peak to peak value, root mean square value and average roughness was calculated using Nova Px software supplied by the NT-MDT, Russia.

Scanning Electron Microscopy analysis was performed on to the Indium tin oxide coated glass. For sample preparation for SEM, dilute solution of Ni-Fe HCFs was drop casted onto the Indium tin oxide coated glass and dried at room temperature. As prepared dried Indium Tin Oxide glass was analyzed by scanning Electron Microscope.

Energy Dispersive Spectroscopy analysis was done with ZEISS SUPRA 40 Scanning Electron Microscope (SEM) coupled to an energy dispersive spectrometer for elemental analysis of samples.

Transmission Electron Microscopy (TEM) analysis was performed using a TECNAI 200 Kv TEM (Fei, Electron Optics). TEM analysis was performed on carbon coated copper grid obtained from M/s. Electron Microscopy Sciences, USA, with the mesh size-400. Ni-Fe HCFs solution was drop casted on the carbon coated copper grid, dried at room temperature and used for TEM analysis.

1.2.4 Peroxidase mimetic activity measurement of Ni-Fe HCFs (1:5)

The peroxidase mimetic activity was done as described earlier elsewhere [(Pandey and Pandey 2013d)]. In a typical situation, the peroxidase like activity of as synthesized Ni–Fe HCFs was determined spectrophotometrically by measuring the formation of the oxidised product of o-dianisidine at 430 nm (ε = 11.3 mM^{-1} cm^{-1}) using a Hitachi spectrophotometer as described earlier [(Pandey and Pandey 2013d)]. Typically, the conversion of o-dianisidine (reduced form, colourless) to o-dianisidine (oxidised form, brown in colour) was measured in 2 ml, 0.1 M phosphate buffer (pH 7.0) containing 15 µl ml^{-1} Ni–Fe HCFs and 50 µM of o-

dianisidine at room temperature with a varying concentration of hydrogen peroxide (0–14 mM). The variation in absorbance as a function of time was monitored at 430 nm (ε = 11.3 mM^{-1} cm^{-1}) and kinetic parameters were calculated as described earlier [(Pandey and Pandey 2013d)].

The steady state kinetics was performed as described earlier [(Pandey and Pandey 2013d)]. In a typical situation, the steady state kinetics was performed by varying the hydrogen peroxide concentration (0-14 mM) at fixed concentrations of o-dianisidine (50 μM). Each reaction was performed in 2 mL phosphate buffer (pH=7.0) and the variation of absorbance was monitored as a function of time at 430 nm (ε= 11.3 mM^{-1} cm^{-2}. The kinetic parameters were calculated by fitting the absorbance data to the Michaelis- Menton equation as described earlier [(Pandey and Pandey 2013d)].

1.2.5 Preparation of modified graphite paste electrode

Active paste of Ni-Fe HCFs was made by mixing 200 μl of solution with 100 mg spectroscopic grade graphite powder. Mixed properly and followed by ultrasonication for 30 minutes and left to dry 60 °C in a vacuum oven overnight. The electrode body used for the construction of graphite paste electrode was purchased from Bioalytical Systems (West Lafayette. IN; (MF 2010). The well of electrode was filled with an active paste of composition of PBNPs 2.5% (w/w), graphite powder 67.5% (w/w), nujol oil 30% (w/w). The desired amounts of modifiers were thoroughly mixed with graphite powder (particle size 1–2 μm) in a blender followed by addition of nujol oil. Finally, the paste surface was manually smoothed on a clean butter paper.

1.2.6 Electrochemical Measurements

All electrochemical measurements were made on a workstation Model CHI660B, CH Instruments Inc., TX in a three electrode configuration with a working volume of 3 ml equipped with an Ag|AgCl electrode (Orion, Beverly, MA, USA) and a platinum plate electrode function as reference and counter electrodes respectively. For normalization, current density in place of current has been taken in respective text. In order to normalize current, optimum current was

divided by electrode active area as reported earlier [(Pandey and Chauhan 2012)]. An analysis of scan rates (ν) dependence on peak current density (j) of the graphite paste electrode was evaluated by recording the cyclic voltammograms at various scan rates from 0.01 V s^{-1} to 0.3 V s^{-1}. All potentials given in the text are relative to the Ag|AgCl. Graphite paste electrode (GPE) worked as a working electrode. Electrochemical sensing of hydrazine was done in 0.1 M $NaNO_3$.

1.3 Results

1.3.1 Synthesis of nanocrystalline Ni-Fe HCFe mediated through $K_3[Fe(CN)_6]$, THF, H_2O_2 and $NiSO_4$

Our previous report revealed that the use of 3-APTMS and cyclohexanone yielded into the formation of processable Prussian blue nanoparticles (PBNPs) which displayed excellent electrochemistry with electron transfer rate constant in the order of 32 s^{-1} representing novel finding on the electrochemical behaviour of a chemically synthesized Prussian blue nanoparticles [(Pandey and Pandey 2013c)]. The similar process also enabled the formation of super peroxidase mimetic mixed metal hexacyanoferrate nanoparticles [(Pandey and Pandey 2013a, d)]. One of the disadvantages of such process is the susceptibility for the formation of –Si–O–Si– linkage as a function of time due to auto-hydrolysis and condensation of 3-APTMS. Accordingly, another novel process justifying the role of tetrahydrofuran hydroperoxide (THF-HP) has been demonstrated for processable PBNPs synthesis [(Pandey and Pandey 2014a)]. Although THF-HP precisely controlled the formation of water soluble PBNPs, the relatively slow process restricted its role for mixed metal hexacyanoferrate synthesis. Further poor commercial availability and relatively tedious synthetic rout of tetrahydrofuran hydroperoxide synthesis itself has been another issue of research task. Obviously the choice of tetrahydrofuran and hydrogen peroxide, both of them are general laboratory reagents, has been another alternative to attempt for the synthesis if these reagents allow controlling the synthesis of mixed metal hexacyanoferrate. As a typical example, we attempted to study tetrahydrofuran and hydrogen peroxide mediated controlled synthesis of Ni–Fe HCF. Accordingly, the suitable concentrations of $K_3[Fe(CN)_6]$, THF, H_2O_2 and $NiSO_4$ were mixed together and

allowed to interact with each other for 30 min at 60 °C in an oven. Indeed, an interesting finding on the formation of water soluble Ni–FeHCF was recorded as shown in Figure.3.1. We also investigated the role of each component on the synthesis of Ni–Fe HCF. In the absence of either THF or hydrogen peroxide, the formation of Ni–FeHCF is not observed under similar condition as shown in Figure.3.1 (A), (B) and (C). All the components present under optimum concentrations yielded into the formation of water soluble Ni–Fe HCF nanoparticles (Figure. 3.1. D).

The next phase of the investigation is to understand the contribution of THF and H_2O_2 during the formation of Ni–Fe HCF which is indicated by an increase in absorbance at 680 nm and decrease in the absorbance at 420 nm (characteristic peaks of potassium ferricyanide) at the fixed molar ratio of Ni–Fe (1:5). Accordingly, we studied the formation of Ni–Fe HCF under different reaction composition: (A) system containing constant concentration of H_2O_2 and Ni–Fe molar ratio and varying concentration of THF and (B) system containing constant concentration of THF and Ni–Fe molar ratio and varying concentration of H_2O_2. The findings are shown in Figure.3.2. and Figure.3.3. with the visual photographs of the respective solutions justified by the variation in the absorption peaks at 420 nm and 680 nm respectively. In system A, variable concentration of THF between 0.125 M and 1.0 M are added into the reaction mixture containing constant concentrations of H_2O_2 (0.7 M) and Ni–Fe molar ratio (1:5) [Figure.3.2]. In system B, variable concentration of H_2O_2 between 0.07 M and 0.6 M are added into the reaction mixture containing constant concentration of THF 1.0 M and Ni–Fe molar ratio (1:5) [Figure.3.3]. The finding revealed that the composition of reacting systems plays a key role during the synthesis of Ni– FeHCF.

This process of Ni–Fe HCF formation could involve the following steps: (i) breakdown of ferricyanide ions leading to the formation of some Fe^{3+} ions and some undissociated ferricyanide ions to obtain Fe^{2+} ions, and (ii) the undissociated ferricyanide ions, Fe^{3+} ions and Ni^{2+} ions lead to the synthesis of Ni–Fe HCF. The new process involves the precise control on the use of Ni–Fe molar ratio for yielding stable water soluble Ni–Fe HCF as shown in Scheme.3. 1.

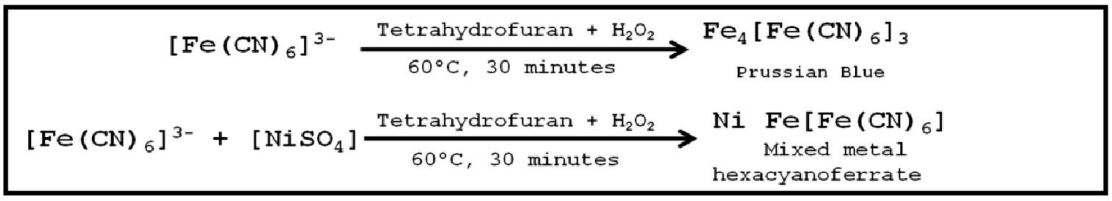

Scheme.3.1. Schematic presentation for the synthesis of Prussian blue and Ni-Fe hexacyanoferrates.

1.3.2 Characterization of Ni-Fe HCFs synthesized through THF, H_2O_2 and $NiSO_4$ (1:5)

The conversion of $K_3[Fe(CN)_6]$ into PBNPs in the presence of tetrahydrofuran and hydrogen peroxide as described in the previous chapter-2 was further explored for the synthesis of controlled synthesis of nickel-iron hexacyanoferrates. In this, nanocrystalline Ni-Fe HCFs with the inherent properties of transition metal analogues was obtained. It was also studied the effect of transition metal on the electrochemical behaviour of PBNPs.

1.3.2.1 Structural characterization

In order to realize the conversion of potassium ferricyanide into Ni-Fe HCFs nanoparticles in the presence of tetrahydrofuran, hydrogen peroxide and nickel ions the images for the synthesis of the solution was observed at first instances. In the presence of optimum concentration of the entire component, the yellow colour solution was turned into blue colour solution.

The importance of the entire component during the synthesis of Ni-Fe HCFs is shown in Figure.3.1 and shows the corresponding vial photographs and UV-Vis spectroscopy. This shows the active involvement of tetrahydrofuran and hydrogen peroxide. Figure.3.1 (A) shows the solution of potassium ferricyanide along with its UV-Vis spectra which shows the absorbance maxima at 420 nm. Figure.3.1 (B) shows the reaction between potassium ferricyanide, hydrogen peroxide and nickel sulphate at 60 °C for 30 minutes and the (B') shows the corresponding UV-Vis spectra which also contains the absorbance maxima around 420 nm. Figure.3.1 (C) shows the reaction between potassium ferricyanide, tetrahydrofuran and nickel sulphate at 60 °C for 30 minutes and (C') shows the

corresponding UV-Vis spectroscopy which also contains absorbance maxima around 420 nm. Figure.3.1 (D) shows the reaction between potassium ferricyanide, tetrahydrofuran, hydrogen peroxide and nickel sulphate at 60 °C for 30 minutes and Figure.3.1 (D') shows the corresponding UV-Vis spectroscopy which contains the absorbance maxima at 680 nm.

The structural characterization of as synthesized Ni-Fe HCFs was done by FT-IR, XRD, AFM, SEM and TEM. Elemental analysis was performed by EDS analysis.

The morphology and thickness of Ni-Fe HCFs has been analyzed by AFM observation. Figure.3.4 shows the typical AFM image of Ni-Fe HCFs illustrating the peak to peak value, root mean square value and average roughness.

As synthesized Ni-Fe HCFs were characterized by FT-IR. Figure.3.5. depicts the FT-IR spectra of Ni-Fe HCFs. The spectrum showed absorption band around 592 cm^{-1}, 2070 cm^{-1}, 1691 cm^{-1}, and 3400 cm^{-1}. As synthesized Ni-Fe HCFs was further characterized by XRD analysis and the spectrogram is shown in Figure.3.6. The four major characteristic peaks are found at c.a. 17.6°, 24.6°, 35.4° and 39.6° (2θ values).

SEM and TEM analysis was done to know the particle size of as synthesized Ni-Fe HCFs. Figure.3.7 shows the SEM image and Figure.3.8. shows the TEM image of Ni-Fe HCFs. The average particle size was found in the order of 31 nm.

Energy dispersive spectroscopy (EDS) is an analytical technique used for the elemental analysis or chemical characterization of a sample. Therefore, EDS study has been attempted for the elemental analysis of Ni-Fe HCFs. Figure.3.9 shows EDS spectra of as synthesized Ni-Fe HCFs nanoparticles. EDS spectra indicate the presence of the characteristic peaks assigned to the carbon, nitrogen, potassium, iron and nickel. The percentage atomic content of these nanoparticles were also shown in the inset of respective figure.

1.3.2.2 Electrochemical characterization of mixed Ni-Fe HCFs nanoparticles

The electrochemical behaviour of mixed Ni-Fe HCFs nanoparticles was studied by cyclic voltammetry (CV). Figure.3.10 summarizes the voltammetric

behaviour of mixed Ni-Fe HCFs of variable Ni:Fe ratio modified electrode in 0.1 M KNO_3 prepared under identical conditions. The presence of well distinct peak at 0.2 V and 0.9 V *vs*. Ag|AgCl were the characteristic of PB [Figure.3.10 (A)]. These peaks can be identified as being due to the redox processes of the outer sphere $Fe^{2+/3+}$ and the inner sphere $[Fe(CN)_4]^{4-/3-}$ couples of PB respectively [(Ricci and Palleschi 2005)]. Similarly, by comparison of the NiHCF peaks with the peaks at 0.65 V, one could assign them to the $[Fe(CN)_6]^{4-/3-}$ transition in the potassium rich form of NiHCF [(Pandey and Pandey 2013a; Prabakar and Narayanan 2008)]. The presence of nickel having Ni-Fe molar ratio in the order of 1:20 notable change in reversible redox behaviour is not observed [Figure.3.10 (B)]. However, an increase in nickel content having Ni-Fe molar ratio in order of 1:10 reveals the occurrence of another reversible peak at 0.46 V *vs*. Ag|AgCl in addition to that of peaks at 0.2 V and 0.9 V *vs*. Ag|AgCl [Figure.3.10 (C)]. When molar ratio of Ni-Fe was 1:5, there are four peaks recorded at 0.20 V, 0.46 V, 0.60 V and 0.90 V *vs*. Ag|AgCl [Figure.3.10 (D)]. Two reversible peaks and a shoulder peaks can be seen at 0.20 V, 0.46 V and 0.6 V respectively in the case of molar ratio of 1:3 [Figure.3.10 (E)]. While for the molar ratio of 1:2, the electrochemical behaviour was dominated by peaks at 0.45 V (larger) and 0.60 V (smaller) *vs*. Ag|AgCl [Figure.3.10 (F)]. As can be seen from the figure, an increase in the nickel concentration significantly alters the electrochemical behaviour of Ni-Fe HCFs. This can be justified by the decrease in the reversible peak at 0.2 V and an increase in the reversible peaks at 0.46 V. At molar ratio 1:2, Prussian blue behaviour was almost diminished showing the occurrence of redox peaks at 0.46 V. These findings revealed the requirement of optimum molar ratio of Ni–Fe at which the both Prussian blue and NiHCF characters could be observed and were found to be 1:5 as shown in [Figure.3.10 (D)] and was used for electrochemical sensing. Additionally, the dependence of electrochemical responses on scan rate for PB, Ni–FeHCF (1:20), Ni– FeHCF (1:10), Ni–FeHCF (1:5), Ni–FeHCF (1:3) and Ni–Fe HCF (1:2) between 0.01 V s^{-1} and 0.3 V s^{-1} in 0.1 M KNO_3 has been recorded as shown in Figure.3.11. As clearly shown in the discussion, there are two well distinguished characteristic peaks at 0.2 V and 0.9 V attributed to PB character. While increasing nickel concentration a new peak is emerging at 0.46 V

and at the Ni–Fe molar ratio of 1:2 the characteristic peaks is almost diminished. At a slow scan rate the peak current is less and while increasing the scan rate the peak currents underwent a gradual increase in all the compositions of Ni–Fe HCF.

1.3.3 Peroxidase like activity of Ni-Fe HCFs nanoparticles (1:5)

Since Ni-Fe HCFs nanoparticles have sufficient stability, an aqueous solution of same may be a potential peroxidase mimetic material. First stage of investigation is to authenticate the peroxidase mimetic activity of mixed metal hexacyanoferrate; as a result, we examined the findings of these issues through the catalytic oxidation of peroxidase substrate o-dianisidine in the presence of H_2O_2. We have examined that the mixed metal analogues also shows the super peroxidase mimetic activity in the presence of mixed metal analogues, hydrogen peroxide and o-dianisidine therefore it is intended to analyze the peroxidase mimetic performance for as synthesized nanomaterial [(Pandey and Pandey 2013d)]. In order to have deeper insight on the kinetic analysis, UV-Vis spectra of the reaction system and spectral change as a function of substrate concentration was studied.

1.3.3.1 Steady state kinetic analysis

1.3.3.1.1 Oxidation of peroxidase substrate o-dianisidine

The UV-Vis spectra of the reaction system containing o-dianisidine, H_2O_2 and Ni-Fe HCFs are shown in Figure.3.12. The results were recorded for varying concentration of H_2O_2. To investigate the apparent steady-state reaction rates, time-scan was started as quickly as possible and the absorbance variation with time was continuously monitored at 430 nm. The kinetic parameter of Ni-Fe HCFs for reaction was evaluated by the initial rate method. The absorbance data were converted to the corresponding concentration term by using the value ε = 11.3 mM^{-1} cm^{-1} (at 430 nm) for the oxidised product of o-dianisidine. Apparent steady-state reaction rates at different concentration for H_2O_2 as a substrate was obtained by calculating the slope of initial absorbance changes with time at fixed concentration of Ni-Fe HCFs nanoparticles. It was found that over a certain concentration ranges of H_2O_2 the plots of initial rate *vs.* H_2O_2 concentration show

typical Michaelis-Menton like behaviour. The enzyme kinetic parameters such as Michaelis-Menton constant (K_m) and maximum initial velocity (V_{max}) were obtained.

1.3.4 Electrocatalytic oxidation of hydrazine over Ni-Fe HCFs (1:5) nanoparticles modified electrode

The oxidation of hydrazine was performed in a 0.1 M $NaNO_3$ solution used as electrolyte solution. The cyclic voltammogram for the oxidation of hydrazine over Ni-Fe HCFs modified electrode are shown in Figure.3.13. As can be seen from the figure, there is an increase in oxidation current around 0.4 V in the addition of hydrazine revealing the catalytic ability for hydrazine oxidation. This finding was further supported by the experimental observation based on amperometry. Figure.3.14 shows the typical amperometric response of Ni-Fe HCFs, on successive additions of hydrazine in 0.1 M $NaNO_3$. Successive additions of hydrazine resulted in a significant increase in the oxidation current, showing the catalytic property of the modified electrode to the oxidation of hydrazine. Figure.3.15 shows the calibration plot of Ni-Fe HCFs system. The calibration plot for hydrazine determination is linear in the range of 0.5 to 2000 μM and the detection limit is 0.05 μM (S/N = 3). The sensitivity for hydrazine analysis was found to be 132.83 μA mM^{-1} cm^{-2} for Ni-Fe HCFs system.

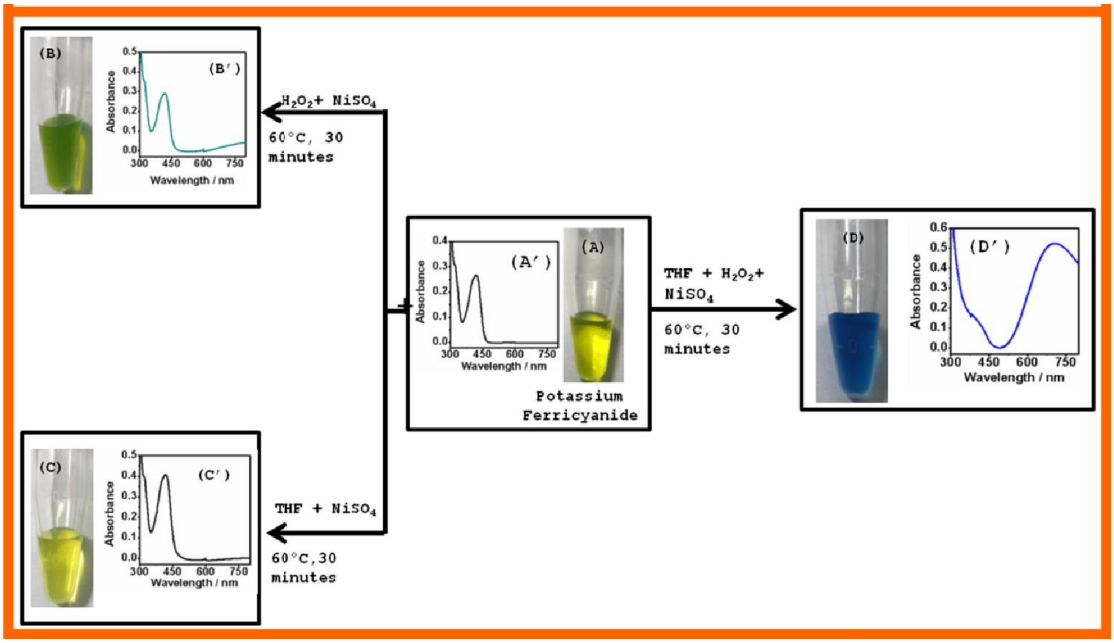

Figure.3.1. Schematic presentation of Ni-Fe hexacyanoferrates formation from THF, H_2O_2 and $K_3[Fe(CN)_6]$ and $NiSO_4$.

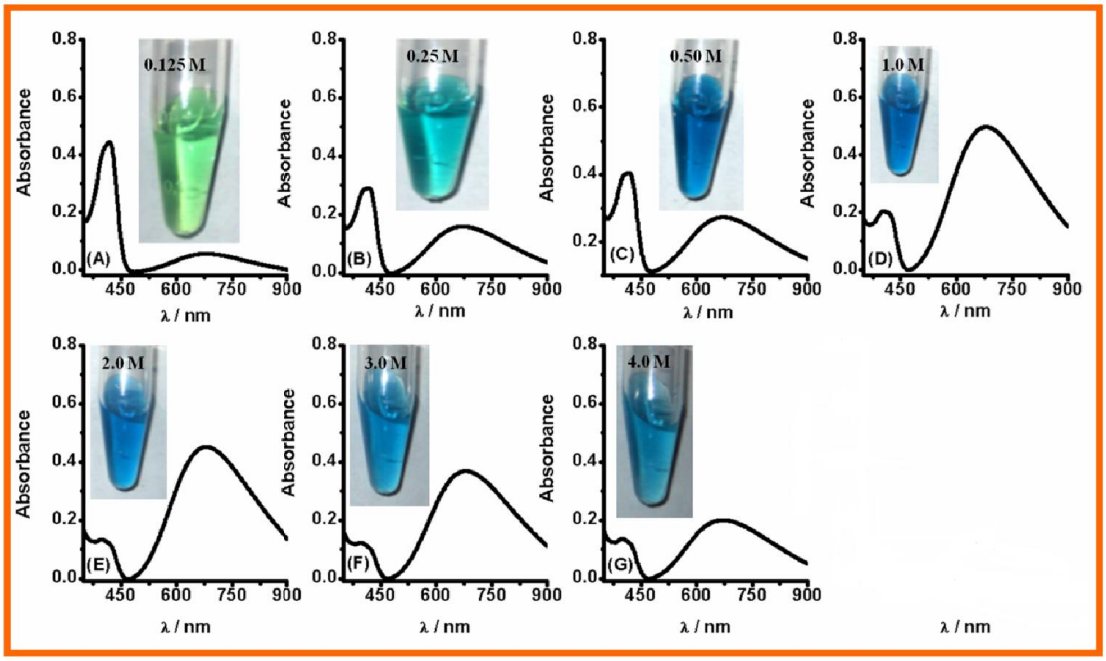

Figure.3. 2. Effect of THF on the formation of Ni–Fe HCF at constant molar ratio of Ni and Fe (1:5) and H_2O_2.

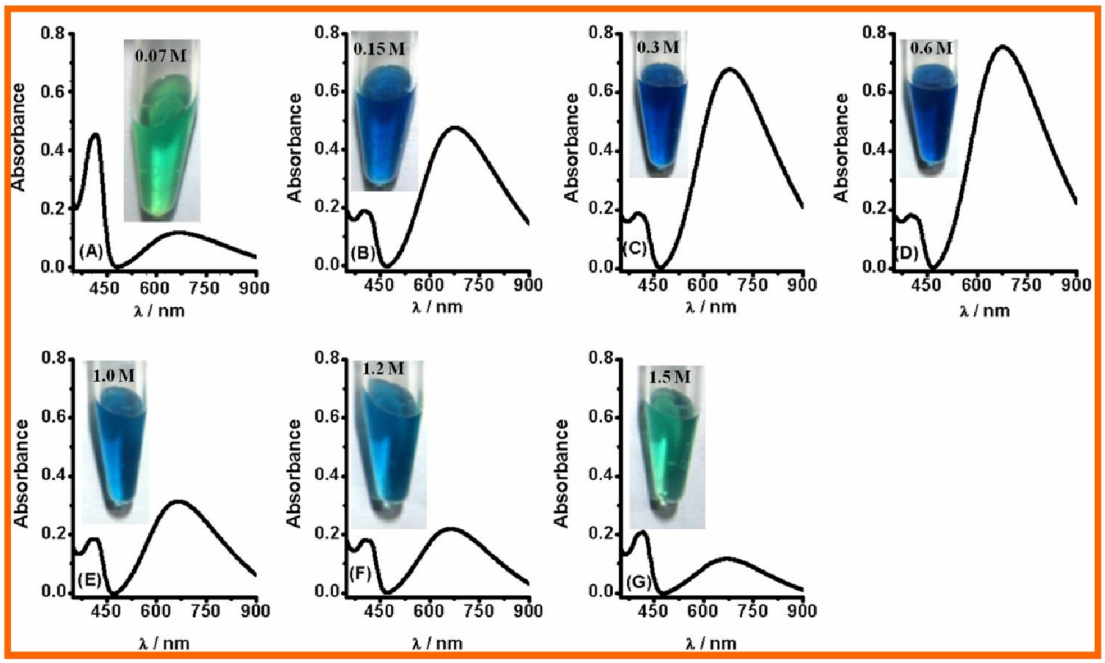

Figure.3. 3. Effect of H_2O_2 on the formation of Ni–Fe HCF at constant molar ratio of Ni and Fe (1:5) and THF.

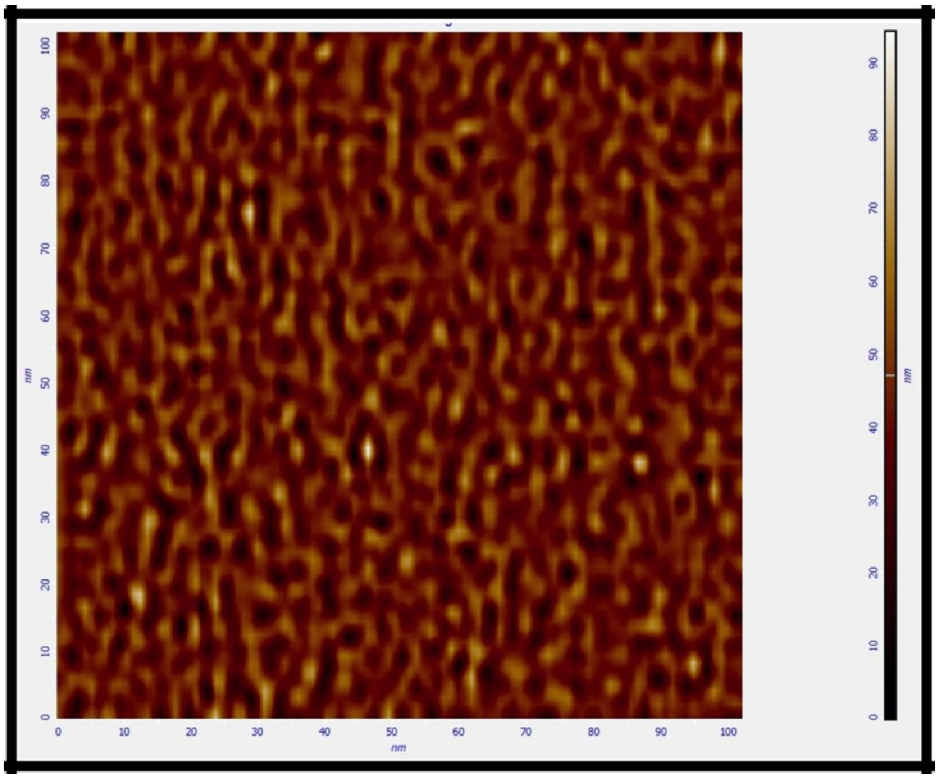

Figure.3.4. AFM image of THF and H_2O_2 mediated synthesized Ni–Fe HCF (1:5).

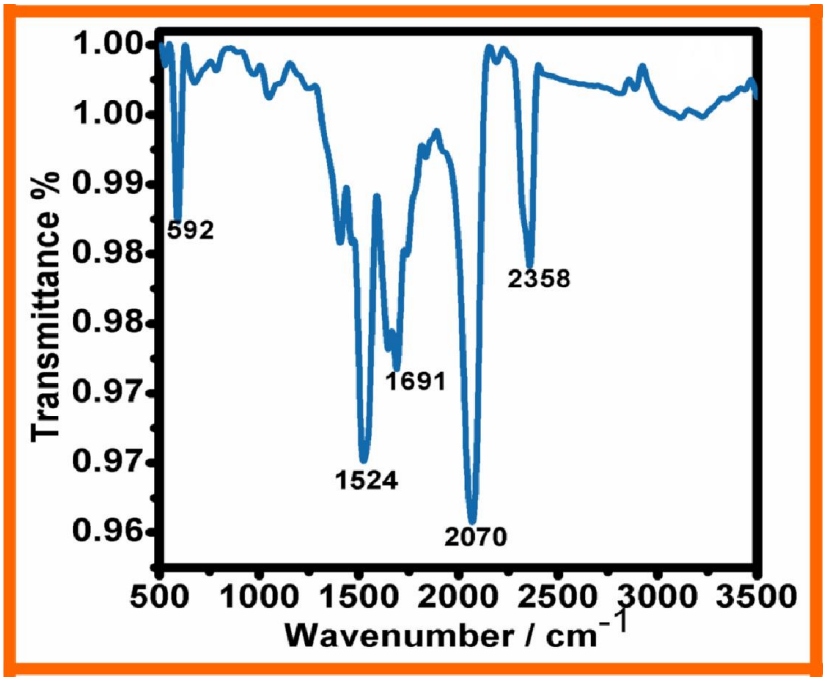

Figure.3.5. FT-IR spectra of THF and H_2O_2 mediated synthesized Ni–Fe HCF (1:5).

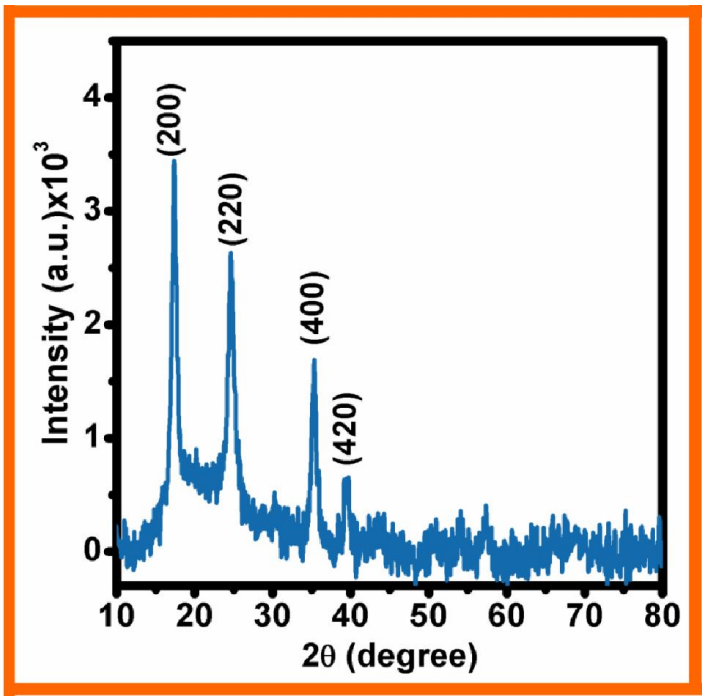

Figure.3.6. XRD analysis of THF and H_2O_2 mediated synthesized Ni–Fe HCF (1:5).

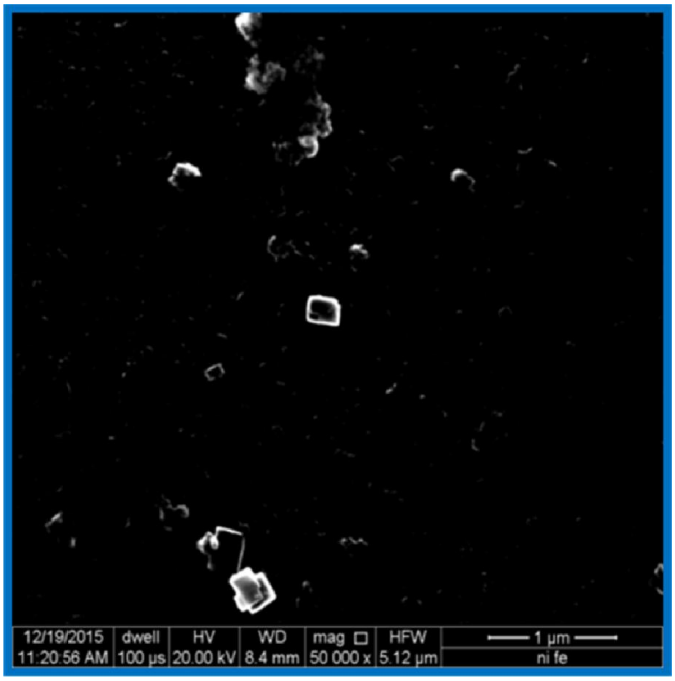

Figure.3.7. SEM image of THF and H_2O_2 mediated synthesized Ni–Fe HCF (1:5).

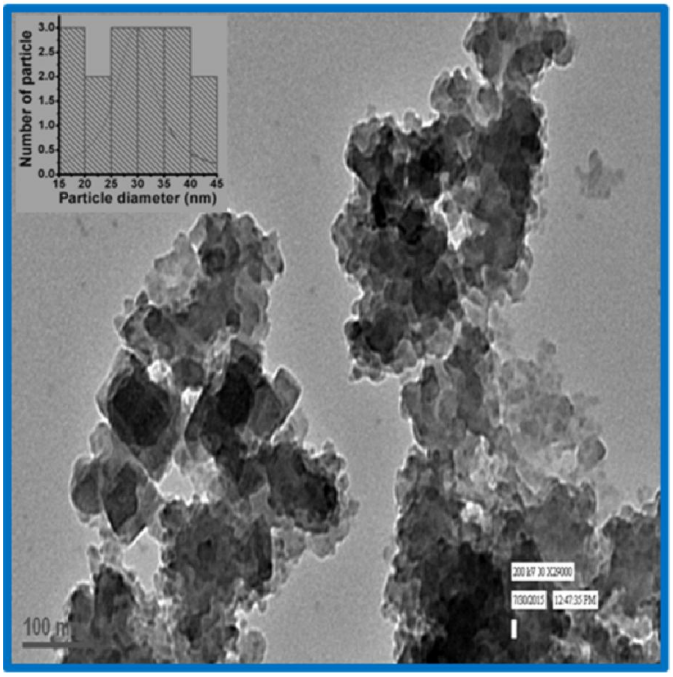

Figure.3.8. TEM image of Ni–Fe HCF (1:5), inset shows the respective size distribution.

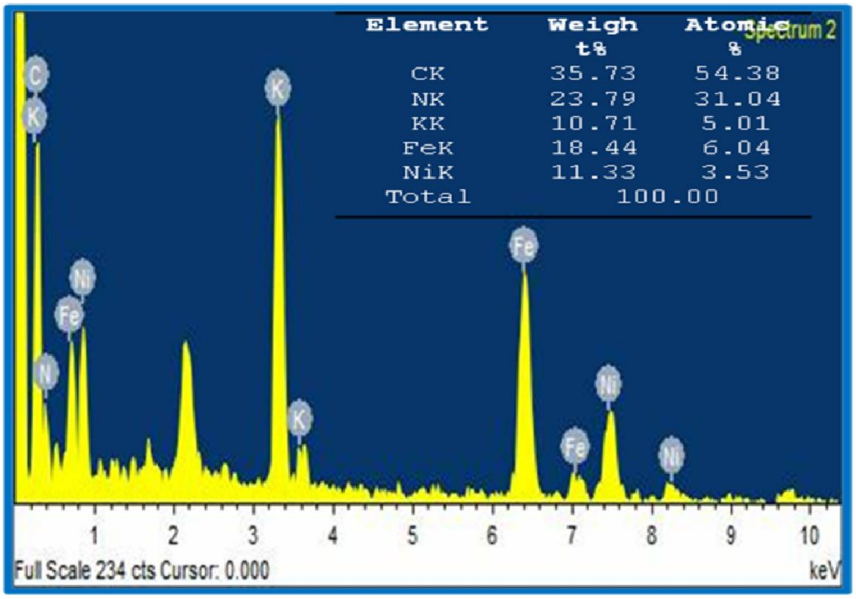

Figure.3.9. Energy dispersive spectroscopy of THF and H_2O_2 mediated synthesized Ni–Fe HCF (1:5). Inset shows the weight %age of EDS analysis.

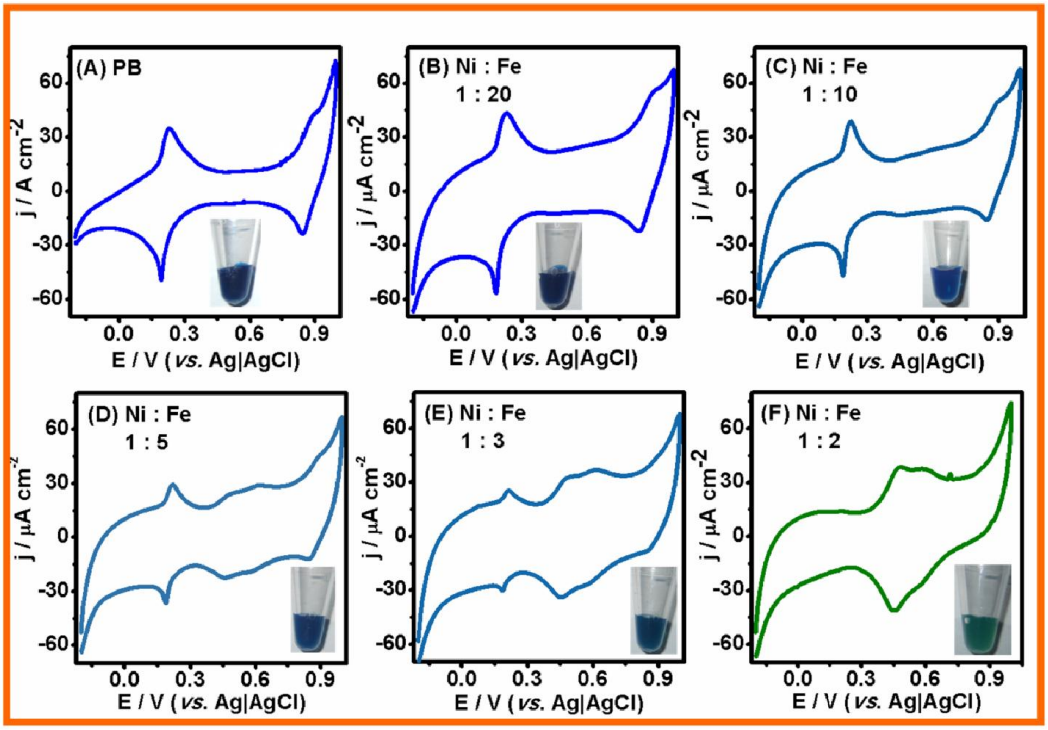

Figure.3.10. Cyclic voltammetric response of THF and H_2O_2 mediated synthesized Ni–FeHCF modified carbon paste electrodes in 0.1 M KNO_3 at a scan rate of 0.01 V s^{-1} made at different Ni:Fe molar ratio: [A] only PBNPs; [B] Ni– Fe HCF (1:20); [C] Ni–Fe HCF (1:10); [D] Ni–Fe HCF (1:5); [E] Ni–Fe HCF (1:3); [F] Ni–Fe HCF (1:2).

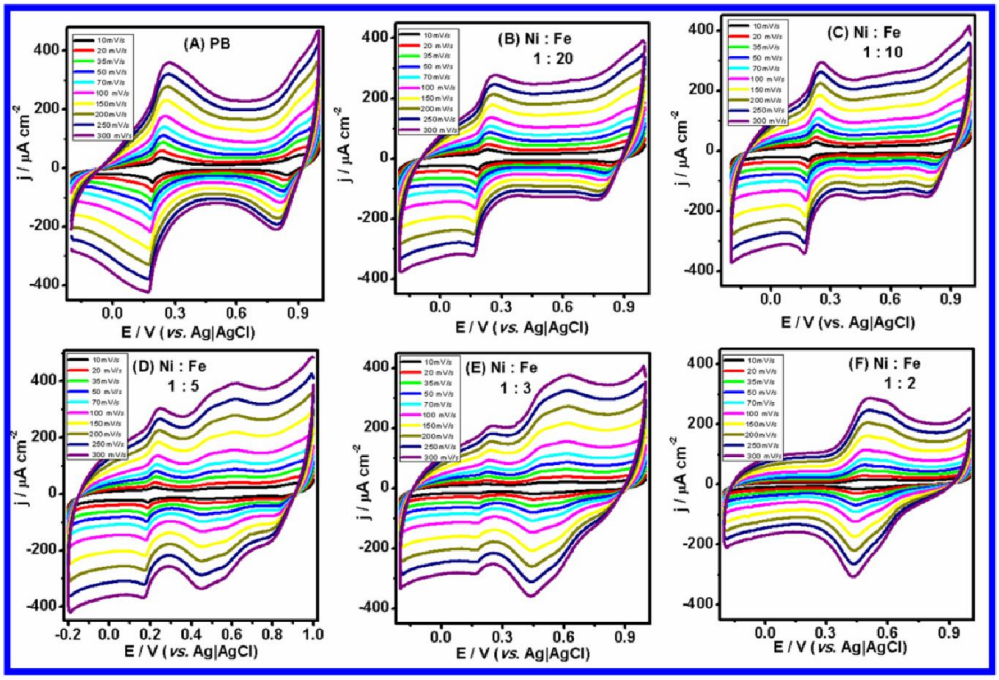

Figure.3.11. Cyclic voltammetric response of THF and H_2O_2 mediated synthesized Ni–FeHCF modified carbon paste electrodes in 0.1 M KNO_3 at different scan rate of 0.01, 0.02, 0.035, 0.05, 0.07, 0.10, 0.15, 0.20, 0.25, 0.35 V s^{-1} made at different Ni:Fe molar ratio: [A] only PBNPs; [B] Ni– Fe HCF (1:20); [C] Ni–Fe HCF (1:10); [D] Ni–Fe HCF (1:5); [E] Ni–Fe HCF (1:3); [F] Ni–Fe HCF (1:2).

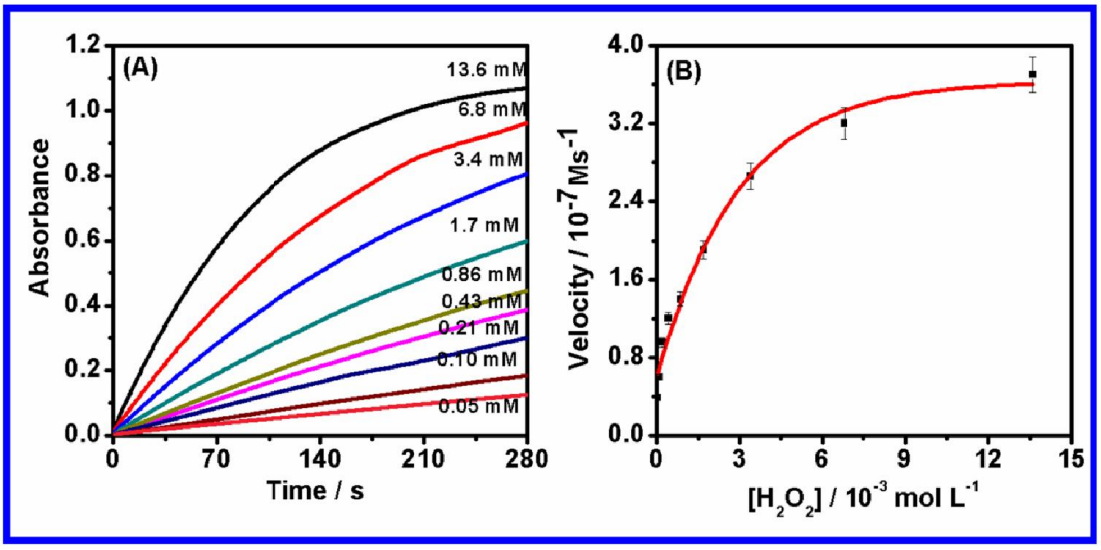

Figure.3.12. (A) Time dependence absorbance changes at 430 nm in the presence of different concentrations (0.05, 0.10, 0.21, 0.43, 0.86, 1.70, 3.40, 6.80 and 13.60 mM) of H_2O_2 and at fixed concentration of o-dianisidine (50 μM) catalysed by Ni–Fe HCF (1:5), and (B) kinetic analysis of Ni–Fe HCF (1:5) with H_2O_2 as substrate.

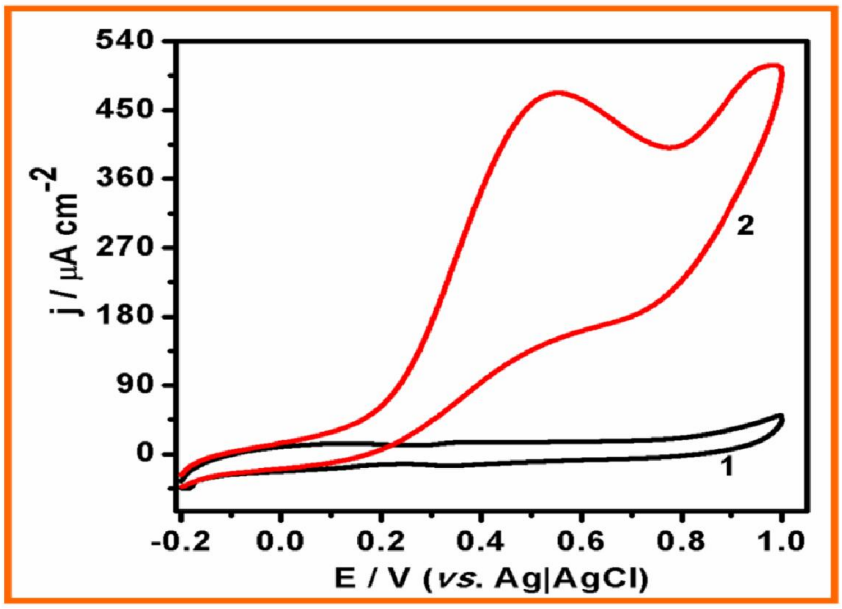

Figure.3.13. Cyclic voltammogram of Ni–Fe HCF (1:5) in the absence (1) and presence (2) of 1 mM hydrazine recorded in 0.1 M $NaNO_3$, pH=7.0 at scan rate of 0.01 V s^{-1}.

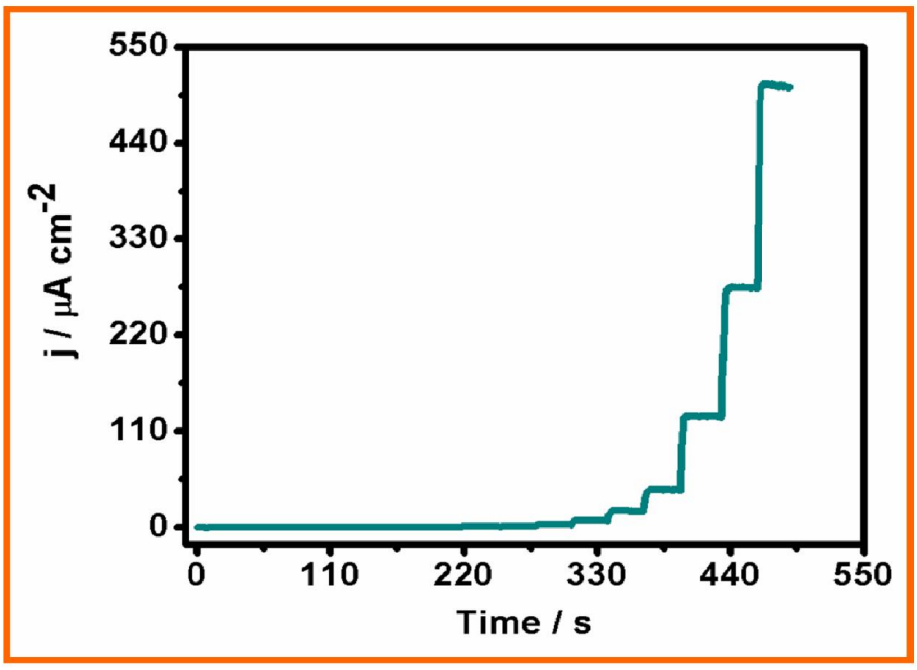

Figure.3.14. Amperometric response of Ni–Fe HCF (1:5) modified electrode on the addition of varying concentration of hydrazine between 0.01 M to 5 mM; operating potential 0.3 V; 0.1 M $NaNO_3$ was the supporting electrolyte.

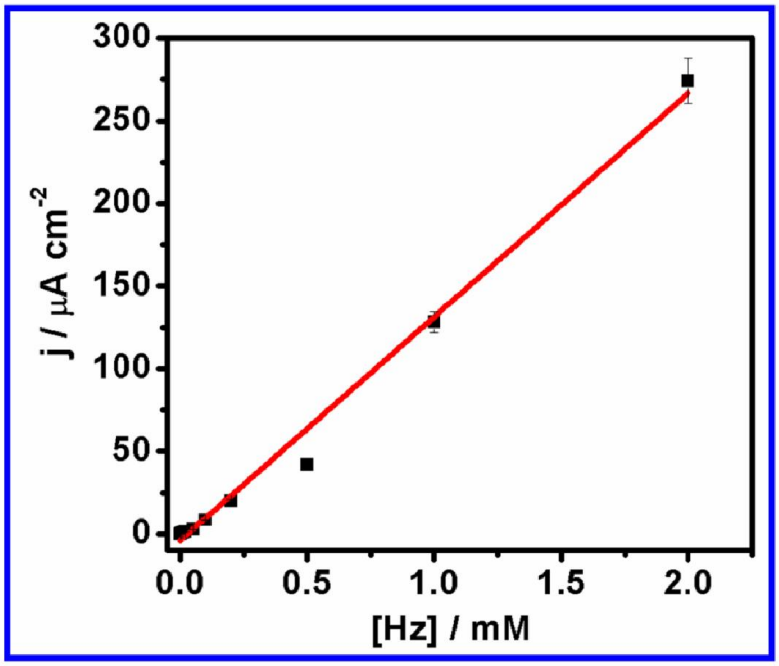

Figure.3.15. Calibration curve for hydrazine analysis.

1.4 Discussion

1.4.1 THF and H_2O_2 mediated synthesis of nanocrystalline Ni-Fe hexacyanoferrates

The challenging requirement of mixed MHCFs synthesis lie in the controlled nucleation of functional PBNPs followed by the simultaneous insertion of the respective transition metal ions during the nucleation and growth of the nanoparticles thereby enabling the precise control of the stoichiometric ratio of two metals in a three dimensional framework having an increased probability for yielding a polycrystalline framework. Such control essentially requires the participation of an organic reagent which is not the precursor of MHCFs and the addition of the same trigger for the nucleation of PB synthesis. When such reagent is mixed with the desired metal ion, the controlled insertion of the respective metal ion within the lattice of the MHCFs is desirable. We found that THF and H_2O_2 is the suitable organic reagent for the synthesis of polycrystalline PB at 60 °C. Therefore, THF and H_2O_2 were further used for the conversion of single precursor $K_3[Fe(CN)_6]$ into the synthesis of their mixed MHCFs. Potassium ferricyanide,

tetrahydrofuran, hydrogen peroxide and nickel sulphate was mixed optimally and keeps it at 60 °C for 30 minutes. The yellow colour solution (absorbance maxima at 420 nm) turned into blue (absorbance maxima at 680 nm) indicated the synthesis of Ni-Fe HCFs. [Figure.3.1.(D)] shows that all the four components at optimum concentration are required for the synthesis of Ni-Fe HCFs. In the absence of any of the component does not lead to the conversion of potassium ferricyanide into Ni-Fe HCFs [Figure.3.1. (B) and (C)]. Important findings recorded during such conversion are as follows: (i) Both THF and H_2O_2 are required for the conversion of $K_3[Fe(CN)_6]$ into Ni-Fe HCFs. (ii) in the absence of any of the reagent does not lead to the synthesis of Ni-Fe HCFs. (iii) optimum concentrations of each component are required for admirable polycrystallinity and electrochemical activity of the nanomaterials.

1.4.2 Structural analysis of Ni-Fe HCFs nanoparticles (1:5)

The conversion of single precursor $K_3[Fe(CN)_6]$ into Ni-Fe HCFs was confirmed by UV-Vis spectroscopy and the visual photographs of corresponding spectra. The structural characterization of as synthesized Ni-Fe HCFs was done by FT-IR, XRD, AFM, SEM and TEM analysis. The electrochemical characterization was performed through cyclic voltammetry.

1.4.2.1 UV-Visible spectroscopy

As shown in Figure.3.1 (D), justified that after keeping reaction mixture at 60 °C for 30 minutes in optimum concentration leads to the decrease at absorbance maxima at 420 nm and an increase in the absorbance maxima at 680 nm which is the characteristic peaks for PB and its mixed metal analogues. The visual photograph are also justified the conversion of single precursor $K_3[Fe(CN)_6]$ into Ni-Fe HCF.

1.4.2.2 Atomic force microscopy (AFM)

Ni-Fe HCFs was characterized by Atomic Force Microscopy and analysed by Nova Px software supplied by NT-MDT, Russia as shown in Figure.3.4. It shows peak to peak value, root mean square value and average roughness in the order of

47.63 nm, 11.72 nm and 9.83 nm respectively which shows the nanogeometrical nature of Ni-Fe HCFs.

1.4.2.3 FT-IR analysis

FT-IR analysis was performed to observe the characteristic peaks of PB and its mixed metal analogues. As shown in Figure.3.5. of the FT-IR spectra of Ni-Fe HCFs revealed the strong absorption peaks at 2070 cm^{-1} which is the characteristic peaks in PB and its mixed metal analogues, corresponds to stretching vibration of –CN group for $Fe^{III}HCF^{II}$ [(Ghosh 1974; Pyrasch *et al.* 2003a)]. The absorption bands near 3400 cm^{-1} and 1691 cm^{-1} are designated to O-H stretching mode and H-O-H bending mode respectively which indicates the existence of interstitial forces of attraction in the sample. The absorption bands around 592 cm^{-1} is due to the structure of Fe^{2+} -CN-Fe^{3+} linkage of FeHCFs.

1.4.2.4 XRD analysis

To know the crystallinity and crystallite size, XRD analysis was performed as synthesized Ni-Fe HCFs. Figure.3.6. shows the X-ray diffractogram of as synthesized Ni-Fe HCFs. XRD analysis shows the four major characteristic peaks which are at c.a. 17.6°, 24.6°, 35.4° and 39.6° (2θ value) those can be assigned as PB phase (200), (220), (400) and (420) [JCPDS file No- 073-0687]. These characteristic peaks are similar to as obtained in PB itself. The crystallite size was calculated by Scherrer formula at their characteristic peaks at 17.6°, 24.6°, 35.4° and 39.6° and the crystallite size were found to be 11.0 nm 8.45 nm, 10.49 nm, and 7.7 nm respectively.

1.4.2.5 SEM and EDS analysis

Figure.3.7 shows the SEM image of Ni-Fe HCFs done on drying the suspension of material on ITO glass. Elemental analysis of the as synthesized Ni-Fe HCFs was performed through Energy Dispersive Spectroscopy (EDS) analysis (Figure.3.9.) justifying the presence of all the necessary component of Ni-Fe HCFs assigned to carbon, nitrogen, iron, and nitrogen.

1.4.2.6 TEM analysis

Transmission Electron Microscopy (TEM) was done to investigate the nanogeometry of as synthesized Ni-Fe HCFs and revealed the average particle size in the order of 31 nm [(Figure.3.8)].

1.4.3 Electrochemical analysis of Ni-Fe hexacyanoferrates

It is necessary to examine the role of mixed metal hexacyanoferrate on the electrochemical behaviour of the same. In line of this, electrochemistry of Ni-Fe HCFs was performed on the graphite paste electrode by cyclic voltammetry in 0.1 M KNO_3 solution. Figure.3.10 shows the cyclic voltammetry of PB and Ni-Fe HCFs of different ratio of Ni and Fe and compared with the PBNPs and NiHCFs as reported earlier [(Pandey and Pandey 2013a)]. As can be seen from the Figure.3.10, an increase in the Ni^{2+} concentration has a significant effect on the CV characteristics of the modified electrode, suggesting an increased amount of NiHCFs in the mixed Ni-Fe HCFs. These findings can be justified by an increase of the peak current at 0.65 V and the decrease in peak current at - 0.2 V and 0.9 V. However, there is a critical concentration of Ni^{2+} in the modifying mixture above which the mixture loses its PBNPs character and retains only NiHCFs behaviour. The results clearly showed that the mixed Ni-Fe HCFs, which contains 1:2 ratio of Ni to Fe, produces electrochemical behaviour of NiHCFs and PB character, is almost vanished. On the contrary, the mixed Ni-Fe, in which the ratio of Ni to Fe is 1:5, retains the electrochemical behaviour of both PB and NiHCFs. Accordingly, the Ni-Fe HCFs made with a molar ratio of Ni:Fe of the order of 1:5 was chosen for structural characterization, practical application in electrochemical sensing and peroxidase mimetic activity measurement as such material yielded both PB and NiHCFs character.

1.4.4 Peroxidase mimetic behaviour of Ni-Fe hexacyanoferrates (1:5)

PBNPs and its mixed metal hexacyanoferrate display analogous behaviour to that of peroxidase and have been studied as potential replacement of peroxidase enzyme which are susceptible for inactivation under variable environmental conditions. Accordingly, there is a potential need of a peroxidase mimetic having

catalytic activity similar to that of peroxidase enzyme. The use of conventional Prussian blue is restricted as peroxidase replacement as such material is not processable in homogeneous assay and display poor catalytic activity as compared to that of peroxidase enzyme. First stage of investigation is to validate the peroxidase mimetic activity of PBNPs and its mixed metal hexacyanoferrates; we examined the findings through the catalytic oxidation of peroxidase substrate o-dianisidine in the presence of H_2O_2. As described earlier, Figure.2.10. represents that colourless o-dianisidine forms a brown product when allowed to react with H_2O_2 and metal hexacyanoferrates and the resulting colour change can be read on a spectrophotometer at a wavelength of 430 nm. The mimetic reaction was further proven by Michaelis-Menton curves. Typical Michaelis-Menton curves can be obtained for the nanodispersion of Ni-Fe HCFs with H_2O_2 as substrate Figure.3.12. The Michaelis constant (K_m) and the maximal reaction velocity (V_{max}) for H_2O_2 was found to be 1.50 mM and 3.07 x 10^{-7} m s^{-1}. K_m is the indicator of enzyme affinity towards substrate. A high Km value indicates weaker affinity whereas a low value suggests a higher affinity. The apparent K_m of Ni-Fe HCFs was compared with HRP, which confirmed that Ni-Fe HCFs shows significant enhanced catalytic behaviour as compared to that of HRP [(Gao *et al.* 2007)]. The operational stability of Ni-Fe HCFs in the physiological pH range are significantly longer for practical applications as this material behaves as a perfect peroxidase replacement to technological development.

1.4.5 Electrochemical sensing of hydrazine over Ni-Fe hexacyanoferrates (1:5) modified electrode

Hydrazine is the starting material in the production of some insecticides, herbicides, pesticide, dyestuffs, and explosive and also used in the preparation of many pharmaceutical derivatives [(Garrod *et al.* 2005; Umar *et al.* 2008; Yin *et al.* 2008)]. Maximum permissible concentration of hydrazine in trade effluents is 3.1 x 10^{-5} M [(Evgen'ev *et al.* 1998)]. Due to this, a reliable technique is required for the selective and sensitive detection of hydrazine. Keeping these in mind, we tried to use the as synthesized material in the chemical sensing of hydrazine in an effective manner. As previously discussed in the electrochemical behaviour of Ni-

Fe HCFs, the molar ratio of Ni-Fe dominantly affects the electrochemical behaviour of Ni-Fe hexacyanoferrates. In that, the molar ratio of Ni–Fe of 1:5 shows the best composition for Ni–Fe HCFs compromising the characteristics of both Prussian blue and nickel hexacyanoferrate character. Therefore, we used this composition of Ni-Fe HCFs in the electrocatalytic oxidation of hydrazine.

Figure.3.13. shows the cyclic voltammograms of Ni–Fe HCF modified electrode in the absence and the presence of 1 mM hydrazine in 0.1 M $NaNO_3$. There is an increase in anodic current close to 0.40 V in the addition of hydrazine revealing the catalytic ability for hydrazine oxidation. The electrocatalytic sensing of hydrazine was made by amperometric analysis under stirred condition. Figure.3.14. shows the amperometric response recorded at 0.3 V *vs.* Ag|AgCl. The calibration curves for hydrazine analysis by amperometry at modified electrodes were constructed using average current recorded for each concentration points and shown in Figure.3.15. The sensitivity of electroanalysis was found in the order of 132.83 μA mM^{-1} cm^{-2} with the lowest detection limit at 50 nM.